Available online at www.sciencedirect.com
ScienceDirect
Ceramics International 38 (2012) 265–270
CERAMICS INTERNATIONAL
www.elsevier.com/locate/ceramint

Effect of Sm_2O_3 on the microstructure and electrical properties of SnO_2-based varistors

H. Bastami, E. Taheri-Nassaj *

Department of Materials Science and Engineering, Tarbiat Modares University, P.O. Box: 14115-143, Tehran, Iran

Received 2 June 2010; received in revised form 7 January 2011; accepted 29 April 2011
Available online 7th July 2011

Abstract

The effect of Sm_2O_3 on the microstructure and non-linear electrical properties of (Co, Nb)-doped SnO_2-based varistors was investigated. The addition of Sm_2O_3 improved the non-linear characteristics of (Co, Nb)-doped SnO_2-based varistors. The threshold electric field (E_B) of SnO_2-based varistors increased significantly from 5340 to 12,460 V cm^{-1} and the mean grain size decreased from 4.7 μm to 1.7 μm as Sm_2O_3 concentration increased up to 0.20 mol%. There was an optimal value (0.20 mol%) of the Sm_2O_3 concentration. The sample doped with 0.20 mol% Sm_2O_3 had the highest non-linear coefficient ($\alpha = 28$). The addition of Sm_2O_3 reduced the relative density of (Co, Nb)-doped SnO_2-based varistors.

Keywords: Varistors; Non-linear electrical behavior; Samarium oxide; Tin oxide; Rare earth; Ceramic

1. Introduction

Tin oxide is an n-type semiconductor with rutile crystalline structure and has many interesting electronic properties. In the recent decades, many papers have been published on new SnO_2-based varistors [1–12]. Tin oxide has very low densification rate due to the dominance of non-densifying mechanisms for mass transport such as surface diffusion or evaporation-condensation. Dense SnO_2-based ceramics can be achieved by introducing dopants (such as CoO, MnO_2) [13] or by hot isostatic processing (HIP). The addition of cobalt oxide creates oxygen vacancies, Co'_{Sn} and Co''_{Sn} defects, which can segregate at grain boundary. Both defects of Co'_{Sn} and Co''_{Sn} can help the formation of Schottky barriers [1–12]. Pianaro et al. [14] found SnO_2-based ceramics doped with 1.00 mol% CoO and 0.05 mol% Nb_2O_5 as promising varistor materials ($\alpha \sim 8$, $E_B = 1870$ V cm^{-1}). A significant increase in α of ~41 and $E_B = 4000$ V cm^{-1} is possible to be achieved by addition of 0.05 mol% Cr_2O_3 [1]. Addition of Cr_2O_3 increases the potential barrier values and the density of states at the grain boundary [1]. It was found that most of rare earth oxides such as Gd_2O_3 [15], Yb_2O_3 [16], CeO_2 [17], Pr_2O_3 [17,18], Dy_2O_3 [19], Er_2O_3 [20] and La_2O_3 [3,4,17,21–23] could significantly improve the non-linear behavior of SnO_2-based varistors similar to that of Cr_2O_3 [1,14]. Oliveira et al. [17] investigated the influence of Pr_2O_3, La_2O_3 and CeO_2 on the structure and electrical properties of (Co, Nb, Cr)-doped SnO_2-based varistors. They reported that Pr_2O_3 and La_2O_3 segregate at the grain boundary and cause a considerable increase of α value (to 62 and 81, respectively). The breakdown voltages of these varistors were 6866 V cm^{-1} and 11,849 V cm^{-1} for Pr_2O_3 and La_2O_3, respectively. They reported that CeO_2 as a dopant did not strongly influence the non-linear values of the SnO_2-based varistors ($\alpha \sim 56$ and $E_B = 5975$ V cm^{-1}) as did La_2O_3 and Pr_2O_3, indicating that CeO_2 could have formed a solid state solution with SnO_2 in the grains, but did not segregate sufficiently at the grain boundary [17]. Also, Oliveira et al. [21] investigated (Co, Nb, La)-doped SnO_2 based varistors and found the values of α and E_B as 46 and 12,432 V cm^{-1}, respectively. Wang et al. investigated the (Pr, Co, Nb)-doped SnO_2 varistors, and reported the non-linear coefficient of 61 and the electric field of 15,400 V cm^{-1} for the varistors doped with 0.15 mol% Pr_2O_3 [18]. Also, Wang et al. [15] reported $\alpha \sim 24$ and $E_B = 11{,}250$ V cm^{-1} for (Co, Nb, Gd)-doped SnO_2-based varistors. They further investigated the effect of La_2O_3 on the non-linear behavior of (Co, Ta)-doped SnO_2 and obtained $\alpha \sim 23$ and $E_B = 6350$ V cm^{-1} [23]. The

* Corresponding author. Tel.: +98 21 82883306; fax: +98 21 82883381.
E-mail address: taheri@modares.ac.ir (E. Taheri-Nassaj).

0272-8842/$36.00
doi:10.1016/j.ceramint.2011.04.139

values of $\alpha \sim 26.3$ and $E_B = 7422$ V cm^{-1} for (Co, Nb, Dy)-doped SnO_2-based varistors were obtained by Wang et al. [19]. Silva et al. [3] reported $\alpha \sim 20$ and $E_B = 4400$ V cm^{-1} for (Zn, Co, Ta)-doped SnO_2 ceramics.

In this paper, the effect of Sm_2O_3 on the microstructure and electrical properties of (Co, Nb)-doped SnO_2 varistors was investigated.

2. Experimental procedures

The varistors were prepared by the standard ceramic technique. Commercial nano-sized SnO_2 powders in the range of 50–80 nm were used (Fig. 1). The molar composition was $(98.95 - x)$ % SnO_2 + 1.00 CoO + 0.05 Nb_2O_5 + x Sm_2O_3 with $x = 0.00$, 0.05, 0.10, 0.20, 0.50, and 1.00 mol%. The oxides used were analytical grade SnO_2 (Merck), CoO (Riedel), Nb_2O_5 (Merck) and Sm_2O_3 (Alfa Aesar). The chemicals were wet milled in ethanol using zirconia balls for 1hr. After drying at 60 °C, the obtained powders were granulated with PVA binder and pressed into the discs with 12 mm in diameter and 1.0 mm in thickness by uniaxial pressing (15 MPa) followed by cold isostatic pressing (CIP) (240 MPa). After burning out of the PVA binder at 650 °C, the discs were sintered in air at 1300 °C for 1 h, and then cooled down to room temperature (5 °C/min). In order to minimize or avoid cobalt loss during the sintering and to ensure the desired composition, the pellets were covered with their own powder. Silver paste was applied on the surfaces of the sintered discs to form electrodes by firing at 600 °C for 10 min.

The apparent density of the sintered samples was measured by the Archimedes method. The crystal structure of the samples was characterized by X-ray diffraction (XRD) (Cu-Kα radiation, Philips X-pert). From the XRD reflections corresponding to the (1 1 0) and (1 0 1) planes, a qualitative analysis of cell distortion in SnO_2 samples was made. The signals were located in the angle values of $2\theta \cong 26.61^\circ$ and $2\theta \cong 33.89^\circ$. The details can be found in [24,25]. The microstructure of the sintered pellets was observed using a TESCAN microscope. The grain size was calculated by the Mendelson equation [26]. I–V characteristics were measured using an ac power supply (Haefely Technology, Model CS 200). The frequency of the ac power supply was 60 Hz. The electrical non-linear coefficient (α) was obtained from:

$$\alpha = \frac{\log(I_2/I_1)}{\log(V_2/V_1)} \quad (1)$$

where V_1 and V_2 are voltages at the currents I_1 and I_2, respectively. The α values were obtained from the curves E–J for current densities chosen between 1 and 10 mA cm^{-2}. The threshold electric field (E_B) was obtained at the current density of 1 mA cm^{-2}.

3. Results and discussion

The XRD pattern of the SnO_2 varistor doped with 0.50 mol% Sm_2O_3 showed that all of the diffraction peaks could perfectly be indexed into a rutile SnO_2 structure (JCPDS card, No. 41-1445). No other phase besides SnO_2 was observed. The amount of additives used was very low and other possible phases may not have been detected because of the detection limit of the XRD equipment. Fig. 2 shows the SEM micrographs of system doped with 0.05 mol% Sm_2O_3. As clearly shown, the microstructure of this system is very simple and contains only one phase (SnO_2 grains). Therefore, no

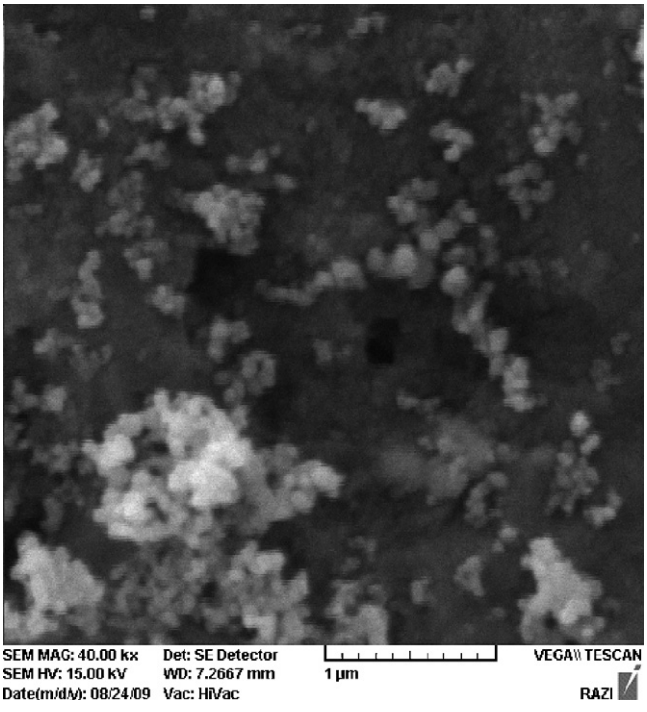

Fig. 1. SEM micrograph of the commercially nano-sized SnO_2 powders.

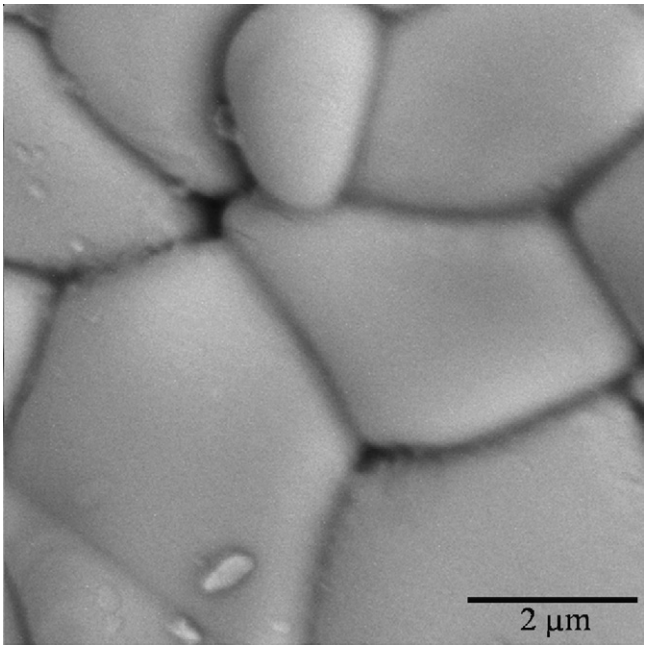

Fig. 2. SEM micrographs of (Co, Nb)-doped SnO_2 based varistor doped with 0.20 mol% Sm_2O_3 sintered at 1300 °C for 1 h.

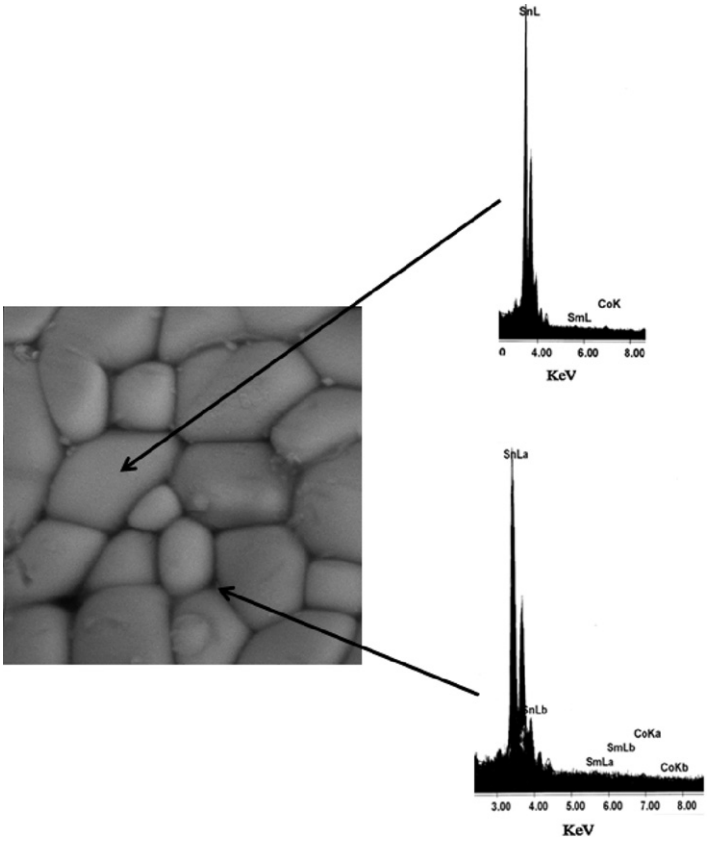

Element	Normalized element analysis (wt%)
Sn	99.81
Co	0.04
Sm	0.14

Element	Normalized element analysis (wt%)
Sn	94.10
Co	2.41
Sm	3.49

Fig. 3. Energy dispersive spectra (EDS) analysis for the sample doped with 0.50 Sm_2O_3 (mol%): grain (point 1); triple point (point 2).

secondary phase precipitated at the grain boundary was observed by XRD or SEM observation. This is in agreement with other studies [1–12,14–24].

Fig. 3 illustrates the energy dispersive spectra (EDS) analyses for the sample doped with 0.50 Sm_2O_3 (mol%) in different regions: grain (point 1), and triple point (point 2). As shown, in the point 1 of Fig. 3, the grains are predominantly composed of SnO_2. The weight percent ratios of Sn, Co and Sm are given in Fig. 3. Little amounts of samarium and cobalt were detected in the grain (Fig. 3, point 1) that could be due to the formation of solid solution in the doped SnO_2-based varistors. The amount of Co and Sm in the point 2 (triple point) increased as compared with the point 1 (grain) that could be attributed to the segregation of cobalt and samarium at this region. The presence of cobalt at the triple point may be due to the formation of a Co_2SnO_4 precipitated phase, Similar to the findings of others [27]. The presence of samarium at the triple point (Fig. 3, point 2) from the EDS analysis could be attributed to the segregation of samarium at the triple point and/or to the formation of some precipitates of $Sm_2Sn_2O_7$.

The characteristics of SnO_2 varistor doped with different molar concentrations of Sm_2O_3 are given in Table 1. The mean grain size of the SnO_2-based varistor without Sm_2O_3 doping was 4.70 μm. This value reduced to1.08 μm for the sample doped with 1.00 mol% Sm_2O_3. So, the addition of Sm_2O_3 reduced the mean grain size of (Co, Nb)-doped SnO_2 significantly and prevented the grains from growing, which is in agreement with the finding of other researchers [1–3,9,10,14–21].

The inhibition of grain growth is believed to occur by a mechanism of solute drag similar to the CeO_2-based ceramics doped with Sm_2O_3. The major driving forces leading to the segregation of an equilibrium concentration of solutes at the grain boundary are: (1) reduction in the elastic strain energy of the crystal lattice due to size difference between the solute and the host atoms for which it substitutes, and (2) the electrostatic

Table 1
Characteristics of (Sm, Co, Nb)-doped SnO_2-based varistors.

Sm_2O_3 (mol%)	0.00	0.05	0.10	0.20	0.50	1.00
Density (g cm^{-3})	6.87	6.84	6.80	6.78	6.75	6.73
Relative Density (%)[a]	98.85	98.42	97.84	97.55	97.12	96.83
Mean grain size (μm)	4.70	2.32	1.96	1.420	1.24	1.08
α	10	17	21	28	16	13
E_B (V cm^{-1})	5340	6750	8470	12,460	10,400	9170

[a]Theoretical density of SnO_2 is 6.95 g cm^{-3}.

potential of interaction between the aliovalent solutes and the charged grain boundary [28–30].

According to Table 1, the addition of Sm_2O_3 reduced the relative density of (Co, Nb)-doped SnO_2-based varistors. This value was 98.85% of the theoretical density (TD) for (Co, Nb)-doped SnO_2 system. The addition of Sm_2O_3 up to 1.00 mol% reduced the relative density to 96.83% TD (Table 1). The increase in porosity is probably due to the segregation of Sm_2O_3 at the grain boundary, hindering the sintering process. Sm_2O_3 appeared to exert an influence on the microstructure of (Co, Nb)-doped SnO_2-based varistors similar to that observed by Pianaro et al. [1] in (Co, Nb, Cr)-doped SnO_2-based varistors.

The threshold electric field versus the current density of the SnO_2-based varistors doped with Sm_2O_3 is illustrated in Fig. 4. As shown, the threshold electric field of the SnO_2-based varistors increased from 5340 to 12,460 V cm^{-1} as Sm_2O_3 concentration increased to 0.20 mol%. The highest non-linear coefficient ($\alpha = 28$) was obtained for the sample doped with 0.20 mol% Sm_2O_3. The improvement of non-linear characteristics of (Co, Nb, Sm)-doped SnO_2-based varistors can be due to the segregation of Sm_2O_3 at the grain boundary, probably inducing electronic interface states that can trap states at the SnO_2–SnO_2 interface. Similar results were found by other researchers in SnO_2-based varistors doped with other transition metal oxides [1–24]. Sm_2O_3 apparently is present at the grain boundary and may alter the potential barrier at the grain boundary, affecting the varistor properties.

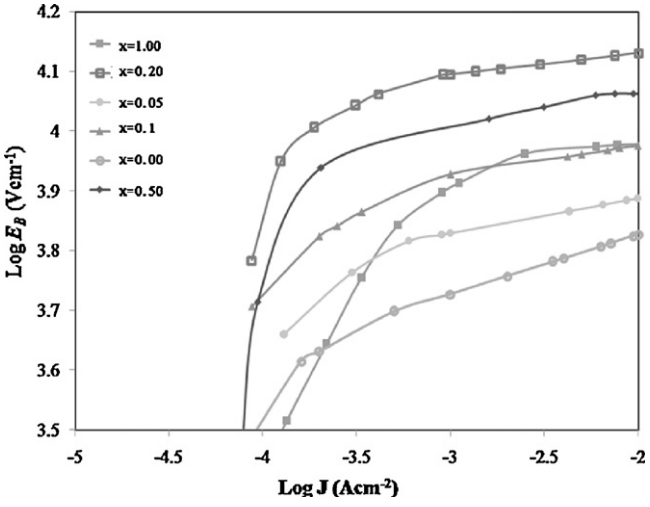

Fig. 4. Applied electric field versus current density for (Sm, Co, Nb)-doped SnO_2 varistors doped with different concentrations of Sm_2O_3.

Addition of Sm_2O_3 in the concentration exceeding 0.20 mol% degraded the non-linear properties of SnO_2 varistors mainly due to the fact that the microstructure of (Co, Nb, Sm)-doped SnO_2-based varistors depended on the concentration of Sm_2O_3. The large amounts of Sm_2O_3 might decrease the grain boundary mobility leading to a decrease in density and consequently, increasing the porosity of (Co, Nb, Sm)-doped SnO_2-based varistors. Also, the higher concentrations of samarium at triple point measured by EDS analysis (Fig. 3, point 2) could be related to the segregation of samarium and/or the formation of $Sm_2Sn_2O_7$ at the triple point. When precipitates are present in higher concentrations at triple points, as in the present case, due to the addition of 0.5 mol% Sm_2O_3, they can affect the nature of SnO_2–SnO_2 junctions and, hence, the number of active barriers. Simões et al. [12] studied the effect of excess precipitates on the non-linear behavior of (Co, Ta, La)-doped SnO_2-based varistors. They proposed that an excessive amount of precipitates may be deleterious to the non-ohmic properties of SnO_2-based varistors because they may create adjacent regions at grain boundary with lower concentrations of segregated metal atoms.

The lattice parameters of undoped and doped SnO_2 with CoO, Nb_2O_5 and Sm_2O_3 determined from the XRD patterns are listed in Table 2. Addition of cobalt increased the lattice volume of SC system in comparison with undoped SnO_2 (Table 2, S system). This could be due to the formation of solid solution. This result is in accordance with the findings of other studies [22,31,32]. Also, the high densification observed in the CoO-doped SnO_2 can be explained by the substitution of Sn^{4+} (0.071 nm) by Co^{2+} (0.078 nm) or by Co^{3+} (0.063 nm) in the SnO_2 crystalline lattice according to:

$$Co_2O_3 \xrightarrow{SnO_2} 2Co'_{Sn} + V^{\bullet\bullet}{}_O + \frac{1}{2}O_2 + 3O^X_O \quad (2)$$

$$CoO \xrightarrow{SnO_2} Co''_{Sn} + V^{\bullet\bullet}{}_O + \frac{1}{2}O_2 \quad (3)$$

According to the above equations, cobalt could stabilize as Co^{2+} or Co^{3+} [1,14,31]. The increase in the lattice volume of un-doped SnO_2 (Table 2, SC system) could be attributed to the stabilizing of cobalt ions as Co^{2+}. The cobalt oxide could influence the adsorption of oxygen species at the grain boundary as represented by the Eqs. (4)–(7) [33]:

$$Co''_{Sn} + \frac{1}{2}O_2 \xrightarrow{SnO_2} Co''_{Sn\bullet}O_{(ads)} \quad (4)$$

$$Co''_{Sn\bullet}O_{2(ads)} \xrightarrow{SnO_2} Co'_{Sn\bullet}O'_{2(ads)} \quad (5)$$

Table 2
Lattice parameters of the sintered samples.

System	Composition (mol%)	$a \pm 0.00001$ (Å)	$c \pm 0.00001$ (Å)	$V = a^2c \pm 0.00001$ (Å^3)
S	100.00 SnO_2	4.73088	3.18186	71.21406
SC	99.00 SnO_2 + 1.00 CoO	4.73088	3.18485	71.28106
SCN	98.95 SnO_2 + 1.00 CoO + 0.05 Nb_2O_5	4.72913	3.18504	71.23238
SCNSm	98.75 SnO_2 + 1.00 CoO + 0.05 Nb_2O_5 + 0.20 Sm_2O_3	4.73063	3.18781	71.33947

$$Co'_{Sn\bullet}O'_{2(ads)} \xrightarrow{SnO_2} Co^{X}_{Sn\bullet}(O)'_{2(ads)} \quad (6)$$

$$2Co^{X}_{Sn\bullet}(O')_{2(ads)} + Co''_{Sn} \xrightarrow{SnO_2} 2Co^{X}_{Sn\bullet}(O'')_{2(structural)} + Co^{X}_{Sn} \quad (7)$$

A decrease in the lattice volume of Co-doped SnO_2 was observed by the addition of Nb_2O_5 (Table 2, SCN system) could be related to the formation of solid solution. This is in agreement with the findings of other researchers [22,31]. The substitution of $Sn^{4+}$by Nb^{5+} can be written as the following reactions [1,14,22]:

$$2Nb_2O_5 \xrightarrow{SnO_2} 4Nb^{\bullet}_{Sn} + V''''_{Sn} + 10O^{X}_{O} \quad (8)$$

$$V''''_{Sn} + 2V^{\bullet\bullet}{}_O \rightarrow 2V^{\bullet\bullet}{}_O + V''_{Sn} \quad (9)$$

$$Nb_2O_5 \xrightarrow{SnO_2} 2Nb^{\bullet}_{Sn} + 2e' + \frac{1}{2}O_2 + 4O^{X}_{O} \quad (10)$$

$$V^{\bullet\bullet} + e' \rightarrow V^{\bullet}{}_O \quad (11)$$

Nb_2O_5 is an electron donor that increases the electrical conductivity of SnO_2. The electrons introduced through Eq. (10) may be involved in the transformation of $V^{\bullet\bullet}{}_O$ into $V^{\bullet}{}_O$ [34].

The increase in both lattice parameters, a and c, in the sample doped with 0.20 mol% Sm_2O_3 (Table 2, SCNSm system) could be attributed to the substitution of Sn^{4+} by Sm^{3+}. Since the ionic radius of Sm^{+3} (0.096 nm) is larger than that of Sn^{+4} (0.071 nm), the substitution of Sn^{+4} by Sm^{+3} as [35]:

$$Sm_2O_3 \xrightarrow{SnO_2} 2Sm'_{Sn} + 3O^{X}_{O} + V^{\bullet\bullet}{}_O \quad (12)$$

leads to the distortion of SnO_2 lattice. Due to the partial substitution of Sn^{+4} by Sm^{+3}, much more Sm_2O_3 will reside at the SnO_2 grain boundary. The species of Sm'_{Sn} segregated at the SnO_2 grain boundary are the origin of the potential barrier. They create oxygen vacancies to promote adsorbed oxygen species formation, which are responsible for the barrier formation near the grain boundary.

Similar to Cr_2O_3, La_2O_3 and other rare earth oxides [3,9,10,23], samarium oxide could react with oxygen species according to the following equations:

$$Sm'_{Sn} + O_2 \xrightarrow{SnO_2} Sm'_{Sn\bullet}O_{2(ads)} \quad (13)$$

$$Sm'_{Sn\bullet} + O_{2(ads)} \xrightarrow{SnO_2} Sm^{X}_{Sn\bullet}O'_{2(ads)} \quad (14)$$

$$Sm^{X}_{Sn\bullet} + O'_{2(ads)} + Sm'_{Sn} \xrightarrow{SnO_2} (Sm^{X}_{Sn})_2O''_{2(ads)} \quad (15)$$

$$(Sm^{X}_{Sn})_2O''_{2(ads)} \xrightarrow{SnO_2} 2(Sm^{X}_{Sn\bullet}O'_{2(ads)}) \quad (16)$$

$$Sm^{X}_{Sm\bullet} + O'_{2(ads)} + Sm'_{Sn} \xrightarrow{SnO_2} (Sm^{X}_{Sn})_2O'_{2(structural)} \quad (17)$$

The role of Co''_{Sn}, Sm'_{Sn}, Sn''_{Sn}, V''''_{Sn} and V''_{Sn} defects (due to the reduction of Sn^{+4} to Sn^{+2} in the interstitial sites) would be related to the increase of the O''_2, O' and O'' adsorbed at the grain boundary interface, causing a decrease in the conductivity of grain boundary by the donation of electrons to the O_2 adsorbed at the grain boundary surface. As pointed out in Ref. [33], the adsorbed oxygen at the grain boundary captures electron from the negatively charged defects at the grain boundary and stays at the interface [33]. In polycrystalline semiconductors, the trapping of electron at the grain boundary has a decisive influence on the electrical transport properties by means of the formation of electrostatic potential barriers [36,37].

Recently, Bueno et al. [38] published a review on the voltage-dependent resistance feature. They discussed completely the details of the basic physical principles involved with the non-ohmic properties of both SnO_2 and ZnO-based non-ohmic systems, with an evaluation of contribution of the dopants to the electronic properties, to the final microstructure and consequently to non-ohmic behavior of the systems. The main conclusion reached by the authors (in the mentioned review) was that despite the significant difference in the microstructure nature of ZnO and SnO_2 varistors, their physical nature is the same that can be described by a Schottky-type double barrier, which is presumed to be associated to oxygen species at the grain boundary of both ZnO and SnO_2-based varistors [36–39]. Glot et al. studied the non-ohmic conduction in SnO_2-based varistors [40,41]. They found high values of the activation energy of electrical conduction and the barrier height in SnO_2-based varistors and concluded the conduction process to be thermally activated not only at low electric field but also at high electric field. This makes possible a simple explanation of the conduction in SnO_2-based varistors as thermoionic emission across a barrier height dependent on electric field [41].

4. Conclusions

The microstructure and electrical properties of (Co, Nb, Sm)-doped SnO_2 based varistors were evaluated. The non-linear properties of (Co, Nb)-doped SnO_2-based varistors increased by the addition of Sm_2O_3. The optimum Sm_2O_3 concentration of (Sm, Co, Nb)-doped SnO_2-based varistors was determined as 0.20 mol%. The highest non-linear coefficient ($\alpha = 28$) was obtained for the sample doped with 0.20 mol% Sm_2O_3. The results indicated that Sm_2O_3 may segregate at the grain boundary, and induce electronic interface states that can trap charge at the SnO_2–SnO_2 interface and lead to the increase of the α value. The threshold field of this sample was 12,460 V cm^{-1}.

References

[1] S.A. Pianaro, P.R. Bueno, E. Longo, J.A. Varela, Microstructure and electric properties of a SnO_2 based varistor, Ceram. Int. 25 (11) (1999) 1–6.

[2] R. Parra, J.E. Rodríguez-Páez, J.A. Varela, M.S. Castro, The influence of the synthesis route on the final properties of SnO_2-based varistors, Ceram. Int. 34 (3) (2008) 563–571.

[3] I.P. Silva, A.Z. Simões, F.M. Filho, E. Longo, J.A. Varela, L. Perazolli, Dependence of La_2O_3 content on the non-linear electrical behavior of ZnO, CoO and Ta_2O_5 doped SnO_2 varistors, Mater. Lett. 61 (2007) 2121–2125.

[4] A.C. Antunes, S.R.M. Antunes, E.R. Leite, J.A. Varela, Effect of La_2O_3 doping on the microstructure and electrical properties of a SnO_2-based varistor, J. Mater. Sci. Mater. Electron. 2 (2001) 69–74.

[5] R. Parra, J.A. Varela, C.M. Aldao, M.S. Castro, Electrical and microstructural properties of (Zn, Nb, Fe)-doped SnO_2 varistor systems, Ceram. Int. 31 (5) (2005) 737–742.
[6] S.R. Dhage, V. Ravi, O.B. Yang, Varistor property of $SnO_2{\cdot}CoO{\cdot}Ta_2O_5$ ceramic modified by barium and strontium, J. Alloys Compd. 466 (2008) 483–487.
[7] F.M. Filho, A.Z. Simões, A. Ries, E.C. Souza, L. Perazolli, M. Cilense, E. Longo, J.A. Varela, Investigation of electrical properties of tantalum doped SnO_2 varistor system, Ceram. Int. 31 (3) (2005) 399–404.
[8] F.M. Filho, A.Z. Simões, A. Ries, I.P. Silva, L. Perazolli, E. Longo, J.A. Varela, Influence of Ta_2O_5 on the electrical properties of ZnO and CoO-doped SnO_2 varistors, Ceram. Int. 30 (8) (2004) 2277–2281.
[9] F.M. Filho, A.Z. Simões, A. Ries, L. Perazolli, E. Longo, J.A. Varela, Non-linear electrical behavior of the Cr_2O_3, ZnO, CoO and Ta_2O_5-doped SnO_2 varistors, Ceram. Int. 32 (3) (2006) 283–289.
[10] F.M. Filho, A.Z. Simões, A. Ries, L. Perazolli, E. Longo, J.A. Varela, Dependence of the non-linear electrical behavior of SnO_2-based varistors on Cr_2O_3 addition, Ceram. Int. 33 (2) (2007) 187–192.
[11] R. Metz, D. Koumeir, J. Morel, J. Pansiot, M. Houabes, M. Hassanzadeh, Electrical barriers formation at the grain boundaries of Co-doped SnO_2 varistor ceramics, J. Eur. Ceram. Soc. 8 (2008) 829–835.
[12] L.G.P. Simões, P.R. Bueno, M.O. Orlandi, E.R. Leite, E. Longo, The influence of excess precipitate on the non-ohmic properties of SnO_2-based varistors, J. Electroceram. 10 (2003) 63–68.
[13] J.A. Cerri, E.R. Leite, D. Gouvea, E. Longo, Effect of cobalt (II) and manganese (IV) on sintering of tin (IV) oxide, J. Am. Ceram. Soc. 79 (3) (1996) 799–804.
[14] S.A. Pianaro, P.R. Bueno, E. Longo, J.A. Varela, A new SnO_2-based varistor system, J. Mater. Sci. Lett. 14 (1995) 692–694.
[15] J.F. Wang, H.C. Chen, W.B. Su, G.Z. Zang, C.J. Zhang, C.M. Wang, P. Qi, (Gd, Co, Ta)-doped SnO_2 varistor ceramics, J. Electroceram. 14 (2005) 133–137.
[16] P. Qi, J.F. Wang, W.B. Su, H.C. Chen, G.Z. Zang, C.M. Wang, B.Q. Ming, (Yb, Co, Nb)-doped SnO_2 varistor ceramics, Mater. Sci. Eng. B 119 (2005) 94–98.
[17] M.M. Oliveira, P.R. Bueno, E. Longo, J.A. Varela, Influence of La_2O_3, Pr_2O_3 and CeO_2 on the non-linear properties of SnO_2 multicomponent varistors, Mater. Chem. Phys. 74 (2002) 150–153.
[18] J.F. Wang, W.B. Su, H.C. Chen, W.X. Wang, G.Z. Zang, (Pr, Co, Nb)-doped SnO_2 varistor ceramics, J. Am. Ceram. Soc. 88 (2) (2005) 331–334.
[19] C.M. Wang, J.F. Wang, W.B. Su, H.C. Chen, C.L. Wang, J.L. Zhang, G.Z. Zang, P. Qi, Z.G. Gai, B.Q. Ming, Improvement in the non-linear electrical characteristics of SnO_2 ceramic varistors with Dy_2O_3 additive, Mater. Sci. Eng. B 127 (2006) 112–116.
[20] P. Qi, J.F. Wang, W.B. Su, H.C. Chen, G.Z. Zhang, C.M. Wang, B.Q. Ming, (Er, Co, Nb)-doped SnO_2 varistor ceramics, Mater. Chem. Phys. 2 (2005) 578–584.
[21] M.M. Oliveira, P.R. Bueno, M.R. Cassia-Santos, E. Longo, J.A. Varela, Sensitivity of SnO_2 non-ohmic behavior to the sintering process and to the addition of La_2O_3, J. Eur. Ceram. Soc. 21 (2001) 1179–1185.
[22] M.M. Oliveira, P.C. Soares-Jr, P.R. Bueno, E.R. Leite, E. Longo, J.A. Varela, Grain-boundary segregation and precipitates in La_2O_3 and Pr_2O_3 doped $SnO_2{\cdot}CoO$-based varistors, J. Eur. Ceram. Soc. 23 (2003) 1875–1880.
[23] C.M. Wang, J.F. Wang, H.C. Chen, W.B. Su, G.Z. Zang, P. Qi, Improvement in the non-linear electrical characteristics of the $SnO_2{\cdot}CoO{\cdot}Ta_2O_5$ varistor material with La_2O_3 additive, Mater. Chem. Phys. 92 (2005) 118–122.
[24] J. Fayat, M.S. Castro, Defect profile and microstructural development in SnO_2-based varistors, J. Eur. Ceram. Soc. 23 (2003) 1585–1591.
[25] B.D. Cullity, Elements of X-ray Diffraction, Addison Wesley, USA, 1978.
[26] M.I. Mendelson, Average grain size in polycrystalline ceramics, J. Am. Ceram. Soc. 52 (1969) 443–446.
[27] J.A. Varela, J.A. Cerri, E.R. Leite, E. Longo, M. Shamsuzzoha, R.C. Bradt, Microstructural evolution during sintering of CoO doped SnO_2 ceramics, Ceram. Int. 25 (3) (1999) 253–256.
[28] J.G. Li, T. Ikegami, T. Mori, Low temperature processing of dense samarium-doped CeO_2 ceramics: sintering and grain growth behaviors, Acta Mater. 52 (2004) 2221–2228.
[29] W.D. Kingery, H.K. Bowen, D.R. Uhlmann, Introduction to Ceramics, Wiley, New York, 1976.
[30] D.D. Upadhyaya, R. Bhat, S. Ramanathan, S.K. Roy, H. Schubert, G. Petzow, Solute effect on grain growth in ceria ceramics, J. Eur. Ceram. Soc. 14 (1994) 337–341.
[31] S.A. Pianaro, P.R. Bueno, P. Olivi, E. Longo, J.A. Varela, Electrical properties of the SnO_2-based varistor, J. Mater. Sci. Mater. Electron. 9 (1998) 159–168.
[32] M.S. Castro, C.M. Aldo, Characterization of SnO_2-varistors with different additives, J. Eur. Ceram. Soc. 18 (1998) 2233–2239.
[33] M.R.C. Santos, P.R. Bueno, E. Longo, J.A. Varela, Effect of oxiding and reducing atmosphere on the electrical properties of dense SnO_2-based varistors, J. Eur. Ceram. Soc. 21 (2001) 161–167.
[34] P. Parra, C.M. Aldo, J.A. Varela, M.S. Castro, The role of oxygen vacancies on the microstructure development and on the electrical properties of SnO_2-based varistors, J. Electroceram. 14 (2005) 149–156.
[35] H. Bastami, E. Taheri-Nassaj, Synthesis of nanosized (Co, Nb, Sm)-doped SnO_2 powders using co-precipitation method, J. Alloys Compd. 495 (2010) 121–125.
[36] P.R. Bueno, S.A. Pianaro, E.C. Pereila, I.O.S. Bulhoes, E. Longo, J.A. Varela, J. Appl. Phys. 84 (1998) 3700–3705.
[37] P.R. Bueno, J.A. Varela, E. Long, Admittance and dielectric spectroscopy of polycrystalline semiconductors, J. Eur. Ceram. Soc. 27 (2007) 4313–4320.
[38] P.R. Bueno, J.A. Varela, E. Longo, SnO_2, ZnO and related polycrystalline compound semiconductors: an overview and review on the voltage-dependent resistance (non-ohmic) feature, J. Eur. Ceram. Soc. 28 (2008) 505–529.
[39] F. Stucki, F. Greuter, Appl. Phys. Lett. 57 (1990) 446.
[40] A.B. Glot, I.A. Skuratovsky, Non-ohmic conduction in tin dioxide based varistor ceramics, Mater. Chem. Phys. 99 (2–3) (2006) 487–493.
[41] A.B. Glot, A.V. Gaponov, A.P. Sandoval-García, Electrical conduction in SnO_2 varistors, Phys. B: Condens. Mater 405(2) (2010) 705–711.